The Importance of Moisture in Hybrid Lead Halide Perovskite Thin Film Fabrication

Giles E. Eperon,[†] Severin N. Habisreutinger,[†] Tomas Leijtens,[‡] Bardo J. Bruijnaers,[§] Jacobus J. van Franeker,[§,#] Dane W. deQuilettes,[∥] Sandeep Pathak,[†] Rebecca J. Sutton,[†] Giulia Grancini,[‡] David S. Ginger,[∥] Rene A. J. Janssen,[§] Annamaria Petrozza,[‡] and Henry J. Snaith*[,†]

[†]Clarendon Laboratory, University of Oxford, Parks Road, Oxford OX1 3PU, United Kingdom, [‡]Center for Nano Science and Technology @Polimi, Istituto Italiano di Tecnologia, via Giovanni Pascoli 70/3, 20133 Milan, Italy, [§]Molecular Materials and Nanosystems and Institute for Complex Molecular Systems, Eindhoven University of Technology, P.O. Box 513, 5600 MB Eindhoven, The Netherlands, [#]Dutch Polymer Institute (DPI), P.O. Box 902, 5600 AX Eindhoven, The Netherlands, and [∥]Department of Chemistry, University of Washington, Box 351700, Seattle, Washington 98195-1700, United States

ABSTRACT Moisture, in the form of ambient humidity, has a significant impact on methylammonium lead halide perovskite films. In particular, due to the hygroscopic nature of the methylammonium component, moisture plays a significant role during film formation. This issue has so far not been well understood and neither has the impact of moisture on the physical properties of resultant films. Herein, we carry out a comprehensive and well-controlled study of the effect of moisture exposure on methylammonium lead halide perovskite film formation and properties. We find that films formed in higher humidity atmospheres have a less continuous morphology but significantly improved photoluminescence, and that film formation is faster. In photovoltaic devices, we find that exposure to moisture, either in the precursor solution or in the atmosphere during formation, results in significantly improved open-circuit voltages and hence overall device performance. We then find that by post-treating dry films with moisture exposure, we can enhance photovoltaic performance and photoluminescence in a similar way. The enhanced photoluminescence and open-circuit voltage imply that the material quality is improved in films that have been exposed to moisture. We determine that this improvement stems from a reduction in trap density in the films, which we postulate to be due to the partial solvation of the methylammonium component and "self-healing" of the perovskite lattice. This work highlights the importance of controlled moisture exposure when fabricating high-performance perovskite devices and provides guidelines for the optimum environment for fabrication. Moreover, we note that often an unintentional water exposure is likely responsible for the high performance of solar cells produced in some laboratories, whereas careful synthesis and fabrication in a dry environment will lead to lower-performing devices.

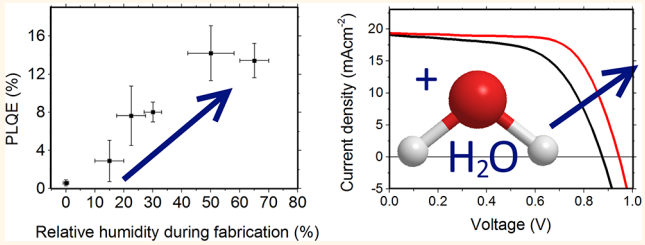

KEYWORDS: perovskite · solar cell · photovoltaics · moisture · defects · humidity · fabrication

The rapid rise in efficiencies of hybrid organic–inorganic perovskite solar cells has led to an explosion of work worldwide on these promising absorber materials. Efficiencies have risen from 3.8% to over 20% certified efficiency in less than 5 years.[1−3] However, most work has focused on optimizing the solar cell constituents, namely, the absorber material and charge-collection layers. The impact of environmental factors on the device fabrication, in contrast, has largely been neglected. The general moisture sensitivity of the perovskite material, in particular, the effect of local humidity during the fabrication of perovskite films, is an important factor which merits further scrutiny. This variable is most often not sufficiently controlled, although recent reports indicate that it may be critical in the formation of high-quality absorber films required for the most efficient devices.[2,4] Indeed, there is a wide variation of atmospheric conditions used between different research laboratories which are often not reported in the literature. While it appears that many groups process their devices inside dry nitrogen-filled gloveboxes, many others fabricate devices in ambient conditions without controlling the humidity, which can vary strongly depending on the local weather conditions at the time. Recent reports have shown that this mostly uncontrolled variable

* Address correspondence to h.snaith1@physics.ox.ac.uk.

Received for review June 15, 2015 and accepted July 31, 2015.

Published online August 06, 2015
10.1021/acsnano.5b03626

could be crucial to attaining the highest efficiencies, so it is likely that a controlled humidity environment is a requirement for optimizing device fabrication.[4−7]

Thus far, there is only a fragmented understanding of the role of humidity with regard to device fabrication and performance due to a lack of thorough and comprehensive studies of this variable. We intend to remedy this by investigating in great detail the impact of moisture on perovskite film properties and photovoltaic performance. We determine that exposure to water at some point in the fabrication of the perovskite film is critical to attain the highest-quality perovskite films, and that device performance improves accordingly.

RESULTS AND DISCUSSION

Photophysics of Dry *versus* Wet Methylammonium Iodide. When considering the role of moisture, it is important to distinguish between formation and degradation of the perovskite film. It appears that the presence of moisture influences the formation of the perovskite film during the crystallization phase but also has a deleterious effect on a fully crystallized film, leading to its degradation. It has been reported by us and others that prolonged exposure to moist air will degrade a methylammonium lead iodide perovskite film.[8−11] The mechanism of degradation is thought to involve the formation of hydrated intermediate structures ($MAPbI_3 \cdot H_2O$ and $MA_4PbI_6 \cdot 2H_2O$), followed by total irreversible degradation to lead iodide. This is clearly of importance when considering the commercial lifetime of a perovskite solar cell exposed to atmospheric conditions. However, during fabrication, the impact of moisture has also been reported to have a critical impact on the crystallization of perovskites. Ko *et al.*, Raga *et al.*, and we have reported that air-annealed perovskite films display efficiencies higher than those annealed in nitrogen, although in these reports, the humidity is not controlled and it can therefore not unambiguously be determined whether oxygen or moisture is responsible for the improved performances.[5−7] The reason for these improvements is thought to mainly stem from an increase in crystal size. You *et al.* have reported that films annealed in controlled levels of humidity (though spin-coated in dry nitrogen) show a maximum performance at 20−40% relative humidity (RH), which in turn is linked to an improved morphology.[4] Notably, Bass *et al.* report that in order to crystallize powders fully, exposure to moisture is crucial.[12] Here, we further delve into the impact of moisture during the preparation of perovskite films and devices and demonstrate that it plays an important role for device performances. To carry out the experiments detailed herein, we built a humidity-controlled chamber, in which humidity can be regulated with a flow of dry nitrogen that passes through a water bubbler. A schematic of the humidity-controlled chamber is shown in the Supporting Information.

An important point of discrepancy between reports of perovskite solar cells is in the preparation of methylammonium iodide (MAI). To the best of our knowledge, throughout the published literature, different degrees of purity of MAI have been used. Many groups recrystallize and wash their MAI crystals to purify them or use the as-formed crystals but do not necessarily remove absorbed moisture from them by stringent vacuum-drying or sublimation. Given that MAI is known to be hygroscopic, as with most alkylammonium salts,[13] MAI that is not treated to remove water will likely contain significant (but uncontrolled) amounts of absorbed water. In order to comprehensively study the impact of moisture on perovskite film formation and properties, here we use a precursor solution prepared from MAI that has been dried overnight in a vacuum oven and subsequently stored in a moisture-free glovebox, so it should be free of most absorbed moisture. We found that we could reversibly hydrate MAI by exposure to air for a day or more, vacuum-drying at 40−50 °C to dehydrate. Approximately, 7 mol % of MAI became hydrated quickly, corresponding to a ∼1% weight increase. We note that in this report we use the nonstoichiometric mixed halide precursor to form $MAPbI_3$ perovskite films, namely, a precursor solution of 3:1 MAI to lead chloride by moles. During annealing, we expect the excess organic and chloride to be removed, as reported by many others.[14−17] This fabrication route is likely to be especially sensitive to moisture during the fabrication, due to the large excess of the hygroscopic MA, and once formed, it should behave similarly to $MAPbI_3$ formed *via* the myriad of other processing techniques.[18]

Initially, we compared the properties of perovskite films prepared with dried and standard MAI powders. The standard MAI is the material normally used in our lab; it is purified after synthesis but not vacuum-dried. It is then stored in ambient air, where it will readily absorb moisture. We fabricated films from the two precursors in identical conditions, annealing the perovskite films at 90 °C for 2.5 h in a controlled humidity environment of 20% RH. In Figure 1a, we show that the morphology of perovskite films fabricated from the two precursors is similar. We can quantify the surface coverages to be 70 and 72% for the standard and dried precursors, respectively. Despite this, the photophysical properties of the films appear to be very different. In Figure 1b, we show that the photoluminescence and photoluminescence quantum efficiency (PLQE) are significantly reduced for the dried precursor, and in Figure 1c, we show that the lifetime of excited species measured with time-resolved photoluminescence is significantly shorter.

The striking difference in physical properties, despite the similar macroscopic morphologies, between the two precursors indicates that the beneficial effect of the absorbed moisture in the standard MAI is not based on a change in macroscopic morphology of the

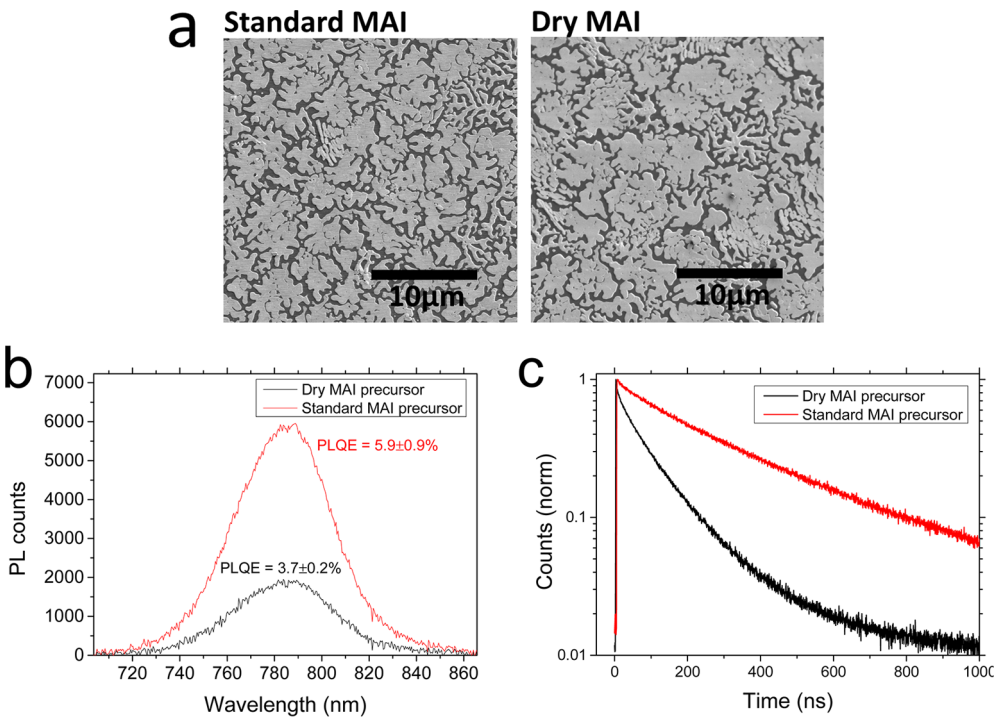

Figure 1. (a) Scanning electron micrograph of the morphology of $MAPbI_3$ films prepared from chloride-containing precursors, using standard and dried MAI powders, in 20 ± 5% RH conditions. (b) Photoluminescence and photoluminescence quantum efficiency, measured using an integrating sphere, for the standard and dried precursor perovskite films. PLQE was measured for at least three points on the sample, and errors represent standard deviation. (c) Time-resolved photoluminescence measured at 785 nm, with excitation at 510 nm, 3 μJ cm^{-2} per pulse, at 1 MHz.

perovskite film. Previously, all differences observed in atmospheres with different relative humidities have been attributed to morphological considerations.

Morphology and Photophysics after Annealing in Different RH. In order to pinpoint exactly how moisture affects the photophysical properties of a perovskite film, we subsequently used only the dry precursor solution for all further experiments. Thus, we are able to explore the effect of exposing perovskite films, which have not already been exposed to water, to different levels of humidity at different stages of their formation.

We investigated the impact that exposure to moisture has on the morphology and physical properties of the perovskite by annealing films in a range of controlled humidity conditions. Typical literature reports indicate that annealing of this perovskite precursor takes ~2−2.5 h to form the best perovskite films.[2,4,19,20]

We noticed that films changed color more quickly in a moist atmosphere, in which they form the final dark film faster. This phase corresponds to the tetragonal $MAPbI_3$ perovskite structure. We quantified this by measuring the *in situ* absorbance of a spin-coated perovskite film over time during the annealing process, while annealing in either dry nitrogen or nitrogen with 30% RH. The films were both spin-coated in a dry nitrogen-filled glovebox to exclude effects during the spin-coating process. We note that, due to the measurement setup, the absorption measured represents two passes of light through the sample.

First considering the film annealed in 0% RH (Figure 2a), we see an initial peak at approximately 410 nm and an absorption feature with onset of ~600 nm. It is not entirely clear which materials are present here, but we propose that lead iodide is responsible for the ~410 nm peak, having been previously observed in the initial stage *via* Raman studies,[16] and possibly a layered-type perovskite, forming due to the large MA excess, could provide the absorbance with onset ~600 nm. This is likely to be the "precursor phase" we have previously assigned through *in situ* X-ray scattering experiments.[21] Upon annealing, we see the absorbance increase steadily, and the characteristic tetragonal $MAPbI_3$ perovskite absorbance spectrum, with onset at ~780 nm, is formed (feature 1 marked on Figure 2a). After ~10 min, the lead iodide peak has disappeared and the perovskite absorbance is maximized. However, we then observe a drop in absorbance around 700 nm, which subsequently increases again until about 30 min, after which time the absorbance remains unchanged up to 180 min of annealing (feature 2 marked on Figure 2a). In Figure 2c, we plot the absorbance at 700 nm as a function of time. The gradual increase of absorbance in the initial phase (t < 10 min) and the subsequent decrease and re-increase (10 < t < 30 min) are clearly seen.

Considering the film annealed in 30% RH (Figure 2b), we notice several differences. First, as soon as the film is

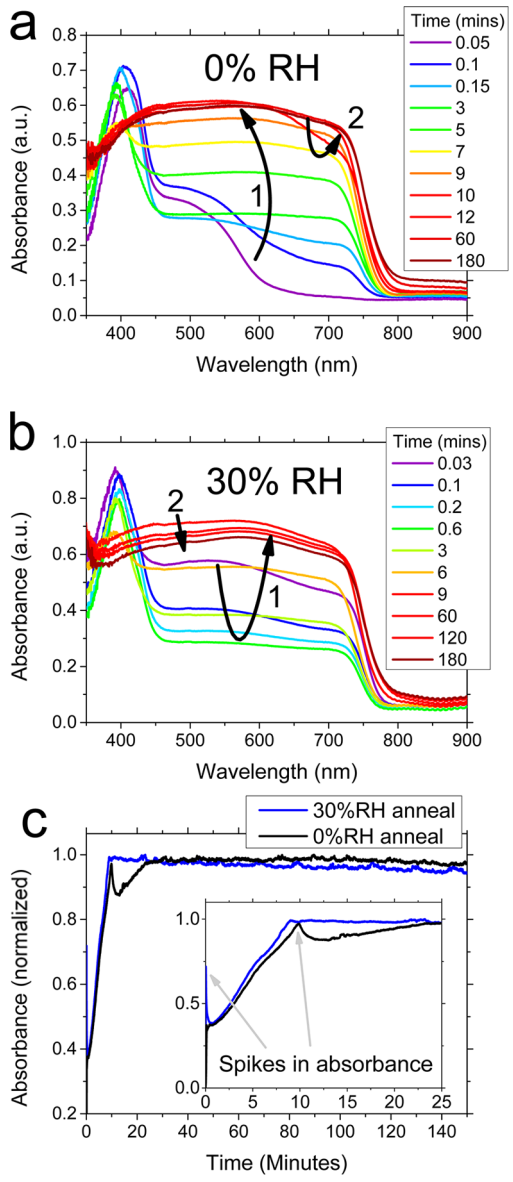

Figure 2. Impact of humidity on rate of perovskite film formation. *In situ* absorbance of a film at different points during the annealing in (a) 0% RH atmosphere and in (b) 30% RH atmosphere. (c) Trace of magnitude of absorbance at 700 nm over time for both films. Inset: Greater detail in the early time period of annealing.

exposed to the moist atmosphere, we observe that the characteristic perovskite spectrum appears very rapidly (see inset of Figure 2c). Upon annealing, this decreases quickly before rising again (feature 1 marked on Figure 2b). The perovskite absorbance is fully formed by ~9 min, much faster than for the 0% RH annealed film, which takes ~30 min. There is no spike and drop, as seen in the 0% RH annealed sample. Upon prolonged annealing, we do observe a drop in magnitude of absorbance in the 30% RH atmosphere, likely indicating a degradation of the perovskite film (feature 2 marked on Figure 2a). This may well be correlated with the formation of the hydrated intermediate structure observed by Yang *et al.*[10]

We note that the absorbance spectrum being maximized does not correspond to the optimum curing conditions for the crystalline perovskite film. Upon being taken from the hot plate and transferred into ambient air, films that are annealed at 90 °C for less time than ~2 h degrade rapidly, forming a transparent material, indicating that there is likely to be a large excess of the hygroscopic MA component remaining; this observed degradation product is in keeping with the hydrated phase observed by Christians *et al.* and Yang *et al.* and can be reversed on heating.[8,10] Additionally, we note that while the quick initial appearance of perovskite absorbance in the humid atmosphere (and subsequent decrease) and the possibly related "spike" in perovskite absorbance in the 0% RH annealed film are likely important, we do not fully understand the significance of this feature and further research on this is necessary. There is significant evidence that intermediate or "precursor" phases are present in many different routes to process high-quality perovskite films.[22−25]

The key conclusion of this experiment is that the final tetragonal $MAPbI_3$ perovskite phase forms faster in a more humid atmosphere. First, we consider the chemistry of the situation. Methylamine and methylammonium halides are soluble in water—hygroscopic, in fact. On the other hand, lead halides, the other component present in the precursor, are insoluble or at best sparingly soluble in water. As such, water acts as a partial solvent for the perovskite precursor—it can solubilize the organic component but not the lead halide. During formation of the perovskite film, in order to form a stoichiometric perovskite, we must retain lead iodide, a stoichiometric amount of methylammonium iodide, and lose a large excess of methylammonium chloride, which is likely driven off as methylamine and hydrochloric acid.[26,27] Hence we would expect the reaction to be accelerated in the presence of moisture, due to the fact that methylamine and hydrochloric acid will form more readily *via* acid−base interaction with moisture, after which they will immediately vaporize, driving the reaction forward. This will allow loss of the methylammonium chloride with lower activation energy, and furthermore, the ambient moisture will provide greater bulk mobility to the methylammonium component retained in the film, reducing the time needed for it to move to form the stoichiometric perovskite crystal. This is in keeping with the observations of Bass *et al.*, who observed a rapid transformation of precursor powders to perovskite powder upon exposure to moisture—the water is solvating the methylammonium and allowing physical material flow to form the perovskite.[12]

We then investigated the impact of a range of humidity levels on the final morphology of the perovskite films, spin-coating and annealing using the dry precursor in different levels of RH. To investigate the

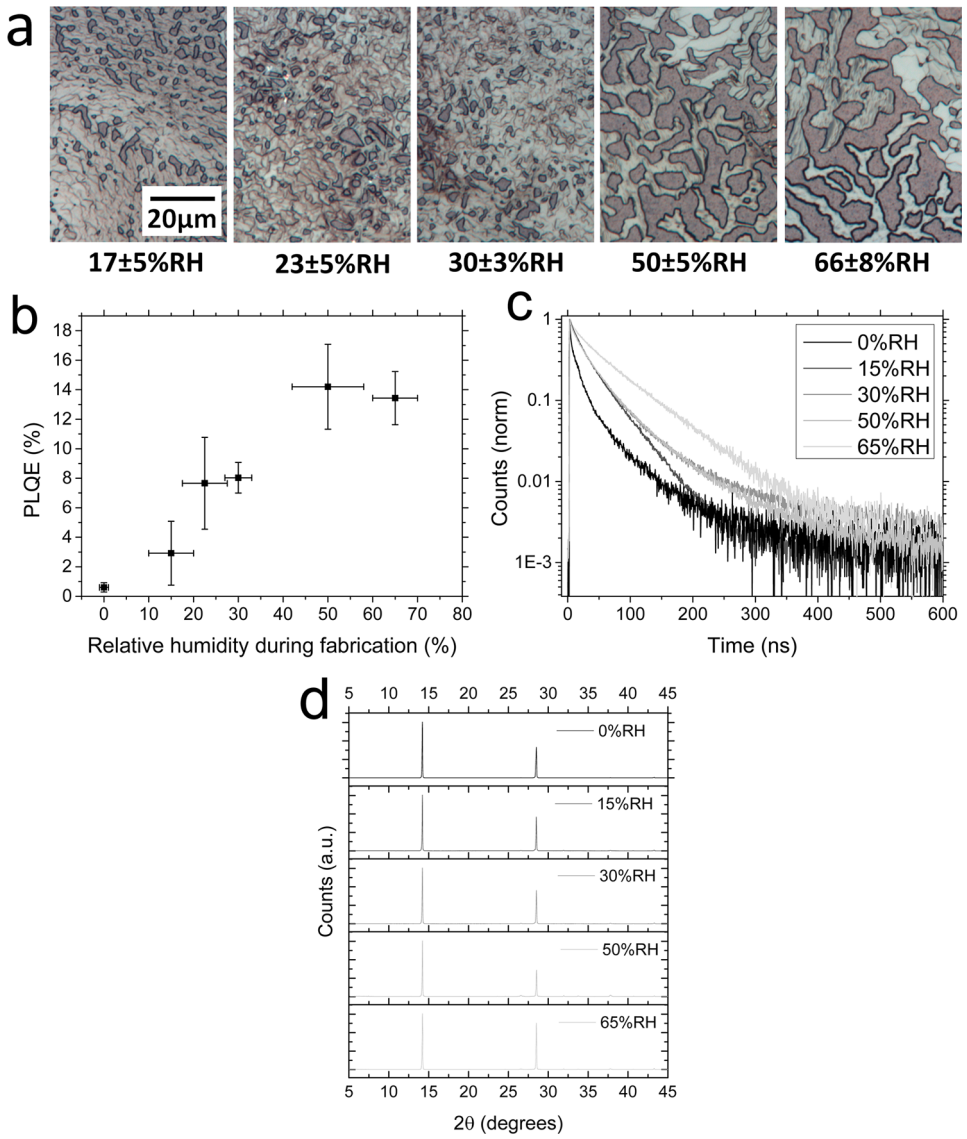

Figure 3. (a) Optical microscope images of perovksite films prepared in different humidity atmospheres on compact TiO_2-coated FTO substrates. The scale is the same in all images. Perovskite material is light in color; bare substrate is darker. (b) Photoluminescence quantum efficiency for perovskite films prepared in different humidity atmospheres. Data points are from the average of at least three measurements each, with error bars indicating standard deviation. (c) Time-resolved photoluminescence measured at 785 nm, with excitation at 510 nm, 3 μJ cm^{-2} per pulse, at 1 MHz, for films prepared in different humidity conditions. (d) X-ray diffraction data for perovskite films prepared in different humidity atmospheres.

morphology, we fabricated films on compact TiO_2-coated fluorine-doped tin oxide (FTO) glass substrates, as used in planar solar cell devices. Different from the inclusion of moisture in the MAI precursor, we do observe a significant change in morphology on varying the atmospheric humidity, as we show in the optical microscope images in Figure 3a. We observe that the best substrate coverage is attained at 30% RH and below, and it worsens with increasing humidity above this level.

Regarding the worsened coverage at higher humidities, there are a number of factors which could be influential. We can envisage that during the spin-coating process, as the solvent (dimethylformamide, DMF) evaporates, the salts or complexes within the solution will start to crash out or precipitate onto the substrate. If the thin wet film is absorbing water as it is losing DMF, then the PbI_2 (or $PbCl_2$) will become increasingly insolubilized and likely to crash out at a faster rate than the MAI. This is likely to induce increased morphological inhomogeneity in the as-cast film. We know from previous work that "dewetting" of the perovskite film into islands occurs due to the growth of large pinholes already present in the as-cast films prior to crystallization.[19,28] Hence, we can infer that the films cast in humid environments are likely to already have larger pinholes present directly after crystallization. If the inhomogeneity of the as-cast film is so extreme that there are regions of neat MACl (or MAI), then these regions could induce dewetting of the perovskite film from the surrounding areas during crystallization.

In addition, the rate of growth and extent of growth of pinholes will be dependent upon how kinetically mobile the components within the perovskite film are during crystallization.[29] If hydration of the material increases the mobility of the ions within the crystallizing film, then this could enable more rapid growth of pinholes. A final consideration is the forces driving dewetting; dewetting occurs due to it being energetically favorable for the perovskite film to reduce its contact area with the substrate, at the expense of increasing its contact area with the environment within which casting is taking place. Having a humid environment is likely to alter both the surface energy of the compact TiO_2 substrate (we note that we observe the same trend on glass) and the perovskite/atmosphere interaction energy.

Beyond looking at the morphological influence of humidity, we also measured photophysical properties, immediately encapsulating films formed on glass with poly(methyl methacrylate) (PMMA) to inhibit contact between ambient moisture and the films. Most striking is the effect of increasing humidity on photoluminescence quantum efficiency (Figure 3b). We observe that films fabricated in higher humidity show increasingly higher PLQE. Films fabricated in a nitrogen-filled glovebox, never exposed to air or humidity, show almost no PLQE, which increases to over 14% for those fabricated in higher humidities. Furthermore, we observed longer-lived photoluminescence decays, meaning that the recombination lifetime of photogenerated charges increases upon an increase in humidity during fabrication (Figure 3c). Additionally, we note that the shape of the decay curves appears to change, which could indicate either a change in the dominating recombination process occurring in films fabricated in the different conditions or a change in the distribution of defects throughout the film.[30,31] We note that morphology, in particular, crystal size, does play a role in determining photoluminescence decay rates for these films, so this is likely to be relevant in addition to the atmosphere-induced changes in the absolute quality of the perovskite material.[32] Previously, it has been shown that larger crystallites display slower recombination rates; however, here, we are not able to accurately extract crystal size. X-ray diffraction spectra, as we show in Figure 3d, for these films show that the highly oriented $MAPbI_3$ phase typical of the mixed halide precursor is formed for all of the humidities, with no significant impurities present. We thus cannot ascribe the enhanced photophysical properties to the measurable formation of lead iodide, previously reported to cause a "self-passivation" of perovskite crystallites when formed by overannealing.[33] We also do not observe any formation of detectable crystalline hydrated intermediates at these conditions.[11]

The strong increase in PLQE and radiative lifetime suggests that the material is suffering from fewer nonradiative losses when formed in higher humidity, suggesting that the material may be of higher quality. We might therefore expect superior performance from a solar cell made from such a material.

Device Performance after Humidity Exposure. The most common device architecture employed in perovskite solar cells relies on a hole-transporting layer of 2,2′,7,7′-tetrakis(*N*,*N*-di-*p*-methoxyphenylamine)-9,9′-spirobifluorene (Spiro-OMeTAD) doped with lithium bis(trifluoromethanesulfonyl)imide (Li-TFSI) coating the perovskite. The doping is achieved by letting Li-TFSI oxidize Spiro-OMeTAD by being in contact with air for several hours, usually overnight.[34] However, we have previously shown that Spiro-OMeTAD is permeable to water and does not constitute a good moisture barrier.[9] Therefore, coating solar cells fabricated in carefully controlled humidity levels with Spiro-OMeTAD and subsequently leaving them overnight in air will likely result in ambient moisture permeating through the Spiro-OMeTAD layer and thus coming into contact with the perovskite film, leading to uncontrolled effects of moisture on the perovskite absorber and invalidating the usefulness of the experiment.

As a means to prevent this uncontrolled exposure of the perovskite to moisture, we employed a moisture-resistant hole-transporting layer comprising a composite of single-walled carbon nanotubes (SWCNT) and PMMA or polycarbonate (PC). As we have previously demonstrated, the polymer matrix can block moisture ingress and subsequent degradation of $MAPbI_3$ perovskites.[9] This makes it the ideal hole-transporting layer to prevent any ambient moisture ingress that may occur after the perovskite layer fabrication. From here, we employ this layer, henceforth referred to as SWCNT-HTL, deposited immediately after perovskite annealing in the relevant humidity atmosphere. In this way, we take the utmost care to *never* unintentionally expose perovskite films to moisture at any stage of the fabrication process.

To determine whether the previous observation of enhanced PLQE when preparing perovskite films in a more humid environment or with a moist (*i.e.*, non-dried) precursor corresponds to improved device performance, we fabricated perovskite solar cells in carefully controlled conditions, immediately sealing with the SWCNT-HTL. We fabricated cells with the dry precursor in a dry atmosphere, with the dry precursor in a moist atmosphere (35 ± 3% RH) and with the standard (moist) precursor in a dry atmosphere. We also fabricated solar cells with the dry precursor in a dry atmosphere, with Spiro-OMeTAD as the hole trans porter, and left them in ambient air overnight to test the hypothesis that moisture ingress through the Spiro-OMeTAD may have an effect. We note that cells fabricated with the SWCNT-HTL and a standard (not dried) perovskite precursor have shown open-circuit voltages and performances very similar to those fabricated

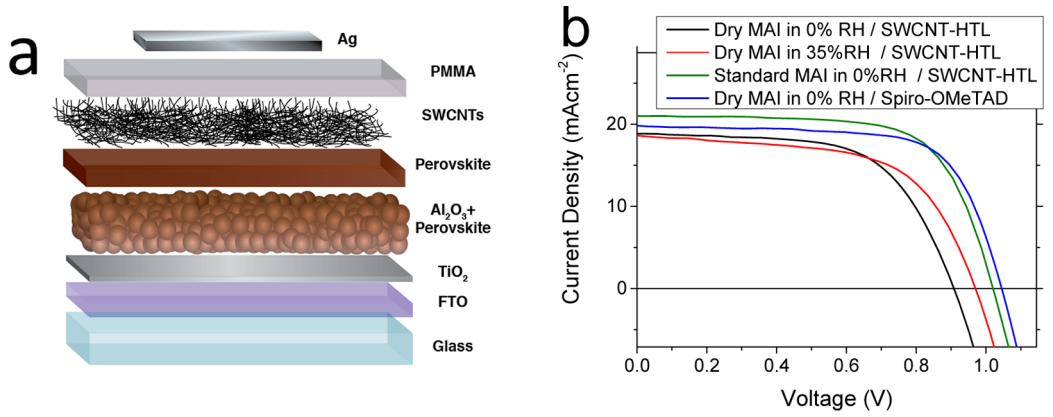

Figure 4. (a) Schematic of the meso-superstructured solar cell architecture investigated. (b) Current−voltage characteristics of meso-superstructured perovskite solar cell devices with and without exposure to moisture in a number of ways, measured under 100 mW cm^{-2} AM1.5 simulated sunlight.

with Spiro-OMeTAD, so we are able to compare devices made with the two hole transporters.[9,35] We also note that all solar cells discussed here are alumina-based meso-superstructured devices, with the device structure shown in Figure 4a. The alumina scaffold negates the detrimental effect of the worsened morphology at higher humidities—it acts to hold the perovskite precursor in place, so there is less unwanted contribution from pinholes reducing voltage, as we have discussed in previous work.[19]

We show current−voltage characteristics from champion cells made in each of these conditions in Figure 4b. As these cells displayed hysteresis in the current−voltage characteristics, we also measured stabilized power output, which along with average device data is given in the Supporting Information. Immediately, we can see that the impact of moisture is quite significant, especially with respect to the open-circuit voltage. Cells made without *any* exposure to moisture show an open-circuit voltage of ∼0.9 V at best. In contrast, when employing the "wet" standard precursor, annealing in a humid environment, or exposing to air with only Spiro-OMeTAD protecting them overnight, we see a large and significant increase in the open-circuit voltage in all these cases. This corresponds to higher power conversion efficiency in most cases, both when measured in a fast current−voltage sweep and in terms of stabilized power output.

From these results, we can conclude that exposure to moisture, which leads to a higher PLQE, also results in devices with a higher open-circuit voltage. This finding is not surprising; from the reciprocity relation described by Rau *et al.*, higher V_{oc} is related to higher luminescence quantum efficiency, due to reduced nonradiative recombination.[5,36,37]

We note that there is a previous report in which air exposure is shown to enhance the performance of a predoped Spiro-OMeTAD-based device (so the oxygen doping *via* ambient exposure was not required).[38] Therein, the authors propose that oxygen may passivate the perovskite surface; our results, in contrast, indicate that it is more likely that the observed improvements can be attributed to the contact with ambient moisture. You *et al.* have previously shown that oxygen does not have the same beneficial effect on photoluminescence properties as moisture;[4] to thoroughly test this possibility here, we also fabricated devices annealed in dry oxygen, and these did not show the same enhancement in V_{oc} or PCE as the moisture-exposed films (see Supporting Information for device data).

In order to understand how detrimental the morphological changes are, regardless of material quality, we also fabricated devices on both planar and meso-structured architectures in a range of humidities, using Spiro-OMeTAD as the HTL and leaving the devices to oxidize Spiro-OMeTAD in ambient atmosphere overnight, in the protocol typical for perovskite solar cell fabrication. Therefore, they are likely to be affected by moisture exposure. We show the device data in the Supporting Information; we observe that planar devices function gradually worse when fabricated in higher humidity, with the lowest humidity being the best, whereas for mesostructured alumina cells, between 0 and 50% RH, device performance is effectively constant, only dropping at humidities above this. This is an important observation for practical reasons: it means that planar devices are dominated by the worsened perovskite morphology, whereas for the mesostructured devices, fabrication is possible without deleterious impact at humidities of up to 50%, likely because the mesostructure holds the perovskite in place, preventing material dewetting during spin-coating and physically preventing shunt diode pathways.

Moisture Post-treatment. On the basis of these results, in particular the enhancement of V_{oc} for the Spiro-OMeTAD-based devices, we realized that we may be able to enhance the properties of a perovskite film by a moisture post-treatment. We made perovskite films in an inert atmosphere, taking the utmost care never to expose them to water, and post-treated them with

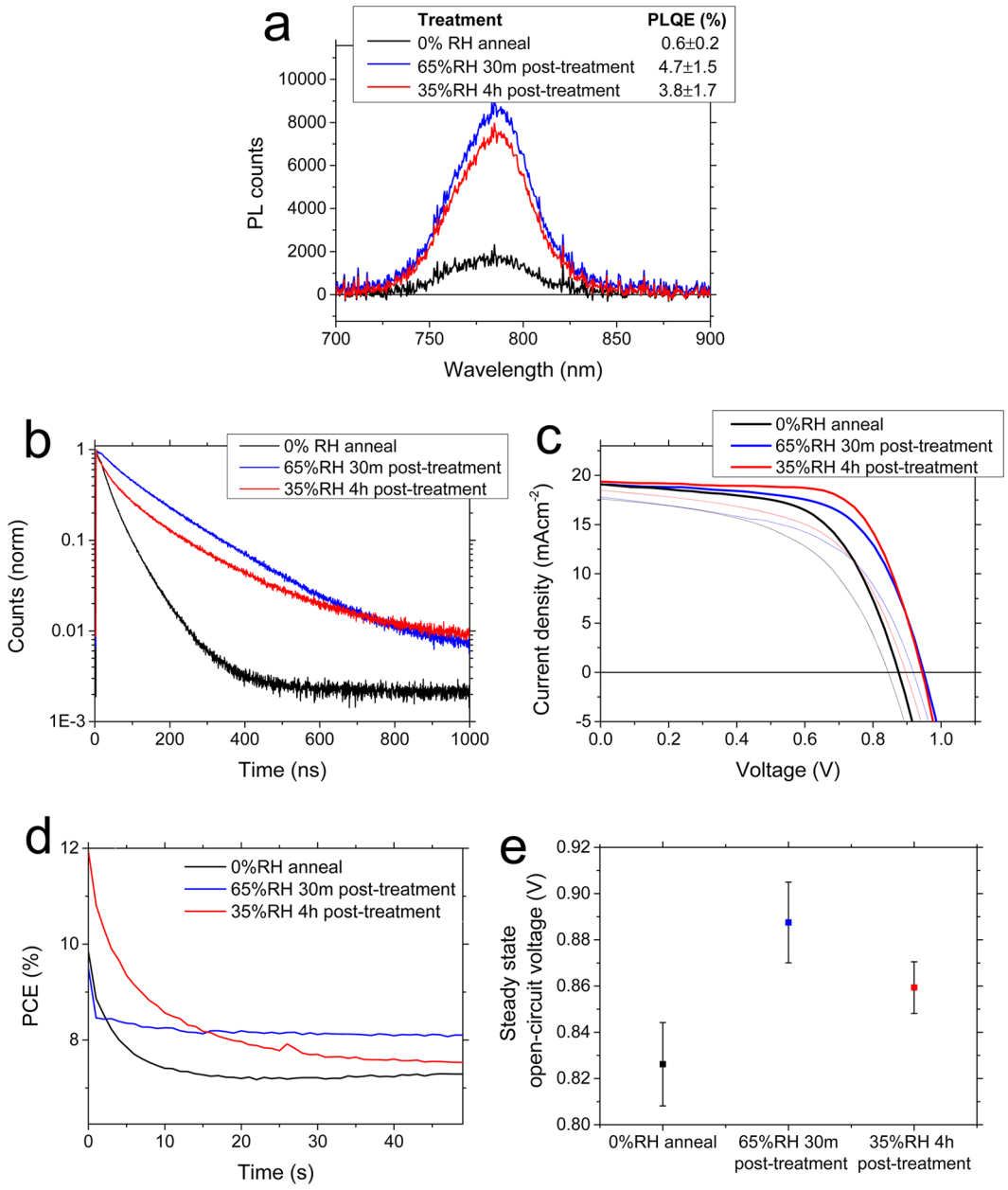

Figure 5. (a) Photoluminescence and photoluminescence quantum efficiency, measured using an integrating sphere, for untreated and moisture-treated perovskite films. PLQE values averaged over at least three measurements are shown in the inset. (b) Time-resolved photoluminescence of untreated and moisture-treated perovskite films, measured at 785 nm, with excitation at 510 nm, 3 μJ cm^{-2} per pulse, at 1 MHz. (c) Current−voltage characteristics of champion devices (bold lines) and average performance (pale lines) for perovskite mesostructured solar cells made with moisture-treated and untreated perovskite films, made with a SWCNT-HTL. (d) Stabilized power output measurements for representative 0% RH annealed and moisture post-treated devices. (e) Steady-state voltage output under 1 sun illumination for moisture-treated and untreated devices (average of five devices each).

water in different ways, subsequently sealing the films with PMMA immediately. We found that we could intentionally enhance the PLQE and photoluminescence lifetime of a film annealed in a dry atmosphere substantially by heating at 90 °C in a 65 ± 5% RH atmosphere for 30 min or by simply leaving the film in 35 ± 5% RH ambient air for 4 h. We show the increases in PLQE and lifetime in Figure 5a and 5b, respectively. In particular, the enhancement in PLQE from 0.6 to 3−5% is notable. We then made photovoltaic devices in 0% RH atmosphere, moisture post-treating some in both ways, and immediately sealing them with the SWCNT-HTL to test whether the PLQE enhancement did indeed correspond to better performance. We show the current−voltage characteristics of champion and average devices for the batch in Figure 4c and Table 1. We observe a significant increase in open-circuit voltage with the moisture post-treatments, showing that we have indeed successfully replicated the effect of fabricating films with unintentional moisture exposure. PCE increased

TABLE 1. Average Device Characteristics Extracted from Current–Voltage Characteristics Measured under AM1.5 100 mW cm^{-2} Illumination for the Devices Described in Figure 5[a]

treatment	J_{sc} (mA cm^{-2})	PCE from JV (%)	V_{oc} (V)	FF
0% RH anneal	17.5 ± 0.8	7.9 ± 1.9	0.85 ± 0.05	0.55 ± 0.07
0% RH anneal + 65% RH 30 min post-treatment	17.8 ± 0.9	9.1 ± 1.9	0.92 ± 0.07	0.55 ± 0.08
0% RH anneal + 35% RH 4 h post-treatment	18.5 ± 0.6	9.4 ± 1.9	0.90 ± 0.06	0.57 ± 0.09

[a] Averages taken for at least 20 devices per treatment.

correspondingly also with the moisture treatments. Since these devices did display current–voltage hysteresis, we show stabilized power measurements in Figure 4d, demonstrating that the moisture post-treatment does result in better stabilized power output than the control samples.

Because the most important and most significant improvement is shown in the open-circuit voltage, to comprehensively demonstrate that voltages measured from current–voltage scans show reliable trends despite the current–voltage hysteresis, we measured steady-state open-circuit voltage for a number of devices under 1 sun illumination, as we show in Figure 5e. We held devices at open circuit until the voltage stabilized (typically within 10–30 s). We observe that the measured voltages are somewhat lower than the fast-scanned open-circuit voltage, but not significantly, and most importantly, the trend still holds, showing that the moisture-treated devices do have a significantly better open-circuit voltage than the untreated ones. Taking all results into account, the 65% RH treatment seems to be somewhat more effective than the 35% RH treatment—open-circuit voltages are higher, stabilized PCEs are higher, and photoluminescent lifetimes and quantum efficiencies are somewhat higher. We note, however, that this treatment required the use of a specialized humidity chamber; the 4 h 35% RH exposure can simply be done in normal lab conditions in many laboratories, and it provides a significant enhancement over the untreated samples.

We can thus confidently conclude that some exposure to moisture enhances the PLQE of a $CH_3NH_3PbI_3$ perovskite film that has not previously been exposed to water. This can either happen unintentionally, as discussed in Figure 4, or intentionally as a post-treatment (see Figure 5). Devices also perform better when they have been exposed to some moisture, mainly due to increased V_{oc}. As discussed earlier, this would be expected for a material with higher PLQE. This highlights a clear conclusion of this study: some moisture exposure (at some stage of the fabrication process) is important for attaining the highest-performing perovskite solar cells. While we have measured only films produced from the nonstoichiometric precursor route, we expect this to generalize to perovskite films formed in other ways, too. We note once more that the precise conditions in which the cells are processed, stored, and tested are not diligently reported in the literature, and our study here suggests that all the highest efficiency cells reported thus far may have a step in the process which involves exposure to an environment containing moisture.

It has recently become apparent that there is often significant inhomogeneity in perovskite films.[31] In order to further investigate the role of the moisture treatments on film quality, we carried out photoluminescence mapping on treated and untreated films to establish whether there was a relation with low or high photoluminescence in particular regions of the film. We measured the spatial photoluminescence intensity distribution at three excitation powers (ranging from approximately 10^{15} to 10^{17} cm^{-3} steady-state charge densities), which we show in Figure 6. We observe that under the lowest intensity, there are many "dark" regions in the 0% RH annealed sample. These are regions where there is likely to be more nonradiative than radiative recombination, which could be an indication of a higher trap density in these regions.[31] In the 4 h 35% RH treated sample, we observe fewer dark regions. To quantify this, we plotted photoluminescence intensity distributions (note that these are normalized to the maximum photoluminescence intensity). We observe that the 4 h 35% treated sample has a distribution tending more toward the highest intensities than the 0% RH annealed sample, confirming our visual analysis that there are fewer "dark", that is, trap-dominated regions. To confirm whether the dark regions have a higher trap density, we can vary the excitation intensity.[30,31] If these regions are trap-dominated because they contain a higher density of traps, an increase in excitation intensity will "fill in" these traps, and the photoluminescence will increase and become more uniformly distributed toward the higher intensities.[30] For both samples, we observe that an increase in intensity reduces the number of dark regions and pushes the photoluminescence intensity distribution toward the higher end of the scale, with the moisture-treated sample having fewer darker regions in all cases. The shifts in distribution to the right with increasing intensity, which imply an increase in uniformity around higher PL, come from the fact that radiative recombination is expected to be bimolecular and should not depend strongly on location,[30,39] while the nonradiative decay is trap-limited and will hence depend strongly on local trap densities.[31] This indicates that

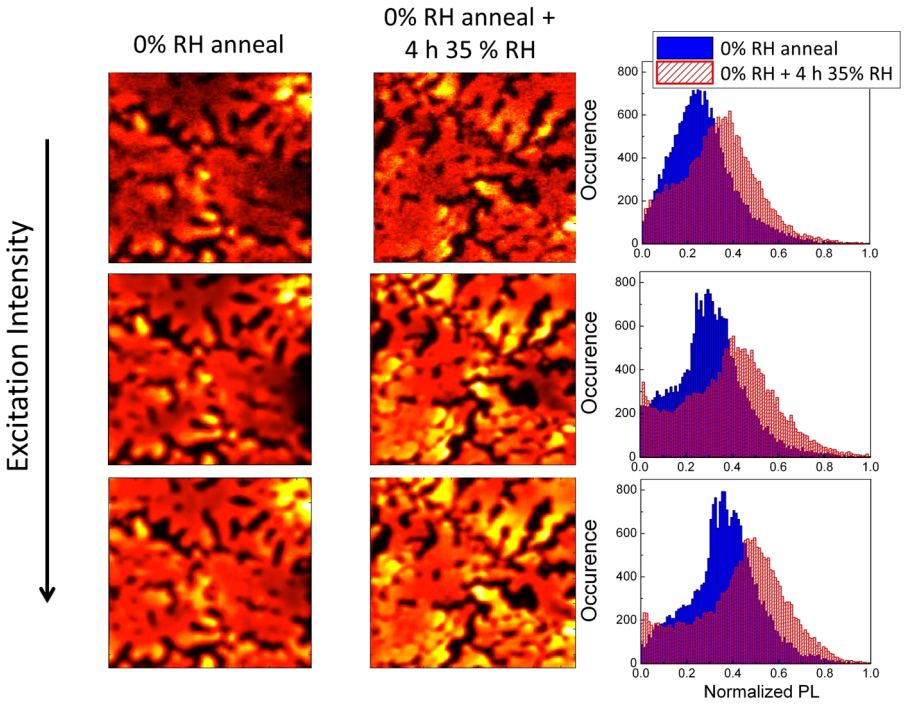

Figure 6. Photoluminescence intensity mapping on 0% RH annealed and 4 h 35% RH post-treated perovskite films. Excitation intensity increases going from top to bottom. Photoluminescence intensity spatial maps are shown on the left; scale is from black (no PL), through red, to yellow (high PL intensity). PL intensity distributions are shown on the right-hand side. In all cases, the field is 100 × 100 μm.

the higher excitation intensity is indeed allowing additional photoexcited carriers to fill in traps and is good evidence that the enhancement in material quality that arises when the perovskite film is exposed to moisture is related to a reduction of trap density in the perovskite film.

Having demonstrated that there is an improvement in perovskite material quality with exposure to moisture, we now need to consider how such an improvement may arise. First, it is important to consider if the improvement is related to the continued presence of moisture adsorbed onto or within the film or as the hydrated phase or if it is a permanent change in the material induced by a moist atmosphere. Previously, it has been shown that the fully hydrated phases can revert to dehydrated perovskite simply by being exposed to dry nitrogen at room temperature.[11] In order to test if the change observed is a permanent or reversible change, we carried out moisture post-treatments on perovskite films prepared in a fully dry atmosphere and then dried some of them out again by heating at 65 °C in a dry nitrogen atmosphere before sealing. In Figure 7, we compare the time-resolved photoluminescence and PLQE of untreated films, moisture-treated films, and those that have been moisture-treated and then dried. We observe that the increased PL lifetime of films that arises upon moisture treatment is sustained after a post-drying step. The PLQE, increased by the moisture treatment, does not return to the very low values of the films never exposed to moisture; within the error margins, it remains unchanged. As such, we conclude that the effect is not simply related to the formation of a layer of hydrated phase perovskite on the surface nor the continued presence of moisture within the film. Furthermore, it is a permanent change—moisture in some way affects the film in a way that is maintained even when moisture is removed. This implies that processing in a humid environment could be a commercially relevant method for improving the quality of perovskite films and not simply an academic curiosity.

Having established that moisture exposure irreversibly improves the perovskite film quality, which we infer to be due to reducing trap state density, we consider the question of how this occurs. Traps in the film can be caused by imperfections in the stoichiometry, such as excess (interstitial) or deficit (vacancy) methylammonium, iodide, or lead atoms or by other lattice defects. It could be suggested that the faster annealing means that the films made in the presence of moisture are subject to more annealing *after* the perovskite has finished forming, and that this enhances the material quality. However, we carried out experiments to show that annealing beyond a certain point, either by increasing temperature or by annealing time, has no beneficial effect on the PLQE of the perovskite film (and is generally detrimental), so we can discard this hypothesis (see Supporting Information). At high enough temperature, the films begin to turn yellow, indicating formation of lead iodide as

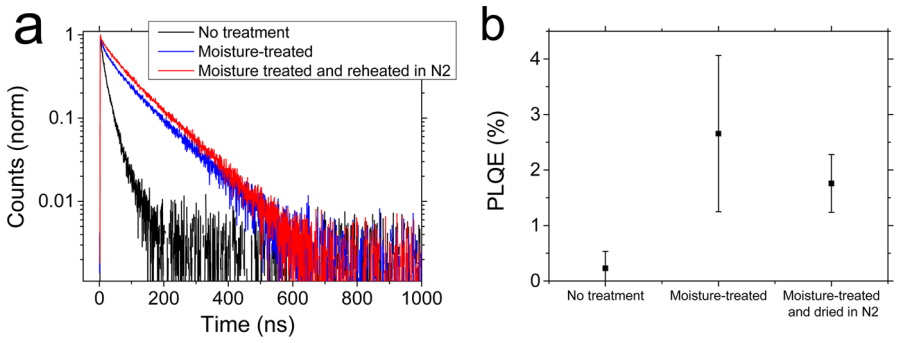

Figure 7. (a) Time-resolved photoluminescence of untreated, moisture-treated, and moisture-treated and subsequently dried perovskite films, measured at 785 nm, with excitation at 510 nm, 3 μJ cm^{-2} per pulse, at 1 MHz. (b) PLQE of films treated in the same ways. PLQE measurements are averaged over six measurements for each treatment; error bars were determined from standard deviation. Films were dried in a nitrogen atmosphere under heating at 65 °C for 1 h.

the perovskite degrades by thermal sublimation of the methylammonium. The increase in PLQE is *only* observed when the film is exposed to moisture in some way. We propose that the presence of moisture affords the reactants greater mobility, as also seen in the rate of formation of the perovskite film, allowing a higher-quality film to result at a fixed temperature.

X-ray diffraction spectra (see Supporting Information) do not indicate any detectable presence of any crystalline material except $MAPbI_3$, so we cannot ascribe the changes to formation of significant hydrate phase or lead iodide at the surface. Furthermore, we do not observe a significant change in the large-scale morphology or grain sizes upon post-treatments with water, as we show *via* scanning electron microscopy in the Supporting Information. Therefore, we also cannot ascribe the improvements to an improvement in large-scale crystallinity or a macroscopic "solvent annealing" effect allowing whole grains to fuse.[4,40]

Having ruled out these options, we propose the following hypothesis: we know that moisture is able to solubilize and remove methylammonium from the perovskite lattice, and we have shown that a film annealed in the presence of moisture forms the perovskite structure faster, implying that water can facilitate the removal of the excess methylammonium in the precursor by partially solubilizing it. Additionally, the reversible formation of a hydrated phase, with water weakly bound to the methylammonium molecules, has been shown.[8] We therefore propose that water can solubilize the methylammonium (and possibly other components), affording it greater mobility and allowing any excesses to be removed and any deficits to be filled in, effectively "healing" the perovskite structure and filling any trap states caused in this way. A reduction of these trap states results in less nonradiative trap-mediated recombination and more radiative recombination. As such, the material quality is improved, PLQE and photoluminescence lifetimes increase, and the V_{oc} and thus PCE attainable in a perovskite solar cell increase.[36] This explanation builds upon that proposed by You *et al.*, who suggested that the enhanced mobility of constituent ions in a moist atmosphere could lead to crystal reconstruction during annealing.[4] They, however, ascribe all observed benefits to the improved morphology; here, we clearly identify that there are more effects at play.

The next question is then whether the effects of the moisture post-treatment could be replicated with other polar solvents, for example, isopropyl alcohol or ethanol, to allow use of a similar post-treatment within moisture-free atmospheres typically used for perovskite processing. In theory, we propose that this should work in a similar manner, and this is currently under investigation.

We note that the perovskites incorporated into the standard solar cells made in our lab, and likely the laboratories of others, already either contain water from nondried MAI or are unintentionally exposed to water *via* an overnight air exposure with only water-permeable Spiro-OMeTAD on top. As such, these cells do not suffer from the V_{oc} limitation and low PLQE that we observe when carefully avoiding water exposure. However, this may not be the case for all perovskite solar cells fabricated in all laboratories. Somewhat counterintuitively, it is, in fact, the most carefully made solar cells (made in a glovebox, with purified and dried MAI) that will suffer from the lack of water exposure. We thus believe that our findings here will provide an extremely important route to improving the performance of such cells and open the way for further studies of the exact mechanism for the improvement upon water exposure.

Furthermore, we note that, although we do see an improvement in device and film performance with the moisture treatments, they are far from perfect. V_{oc} is not improved to the extent that it is by using our "standard" moist perovskite precursor, and PLQE remains far from the highest reported values. We therefore conclude that other additional treatments are probably necessary for a perovskite film to achieve its full potential in a controlled manner. Some work has already been carried out to investigate what role additives, in the broadest sense, can have on the

crystallization and quality of perovskite films, which is likely to be a promising avenue for increasing the PCE to the highest values possible.[41,42] As an aside, we also note that Sn-based perovskites, such as $CH_3NH_3SnI_3$, degrade very rapidly when exposed to any atmosphere and thus cannot benefit from this advantageous moisture exposure. Fully understanding the mechanism and replicating it with alternative less degrading solvents may thus prove to be critical to advance Sn-based perovskite research.

CONCLUSION

We have demonstrated the critical role of moisture exposure during metal halide perovskite thin film fabrication on the material quality. Moisture exposure results in higher open-circuit voltage in photovoltaic devices, higher photoluminescence, and longer photoluminescence lifetimes. We have determined that this likely stems from a reduction in trap state density, which we postulate to be enabled by the partial solvation of the methylammonium component. We note that often moisture exposure can be unintentional, occurring during the Spiro-OMeTAD doping stage or residually in the precursor solution. However, careful synthesis and fabrication in a dry environment will result in lower material quality and worse-performing films. We provide guidelines for the optimum environment for film fabrication and show that a moisture treatment after film fabrication can improve film quality in the same way. These results are crucial for the understanding of the field, in general, and enabling the community to understand the best way in which to produce a perovskite film. They should pave the way for fabrication of high-performing devices and further studies on the exact mechanism of improvement upon moisture exposure.

EXPERIMENTAL SECTION

Materials. Unless otherwise stated, all materials were purchased from Sigma-Aldrich or Alfa Aesar and used as received. Spiro-OMeTAD was purchased from Borun Chemicals.

Perovskite Precursor Preparation. MAI was synthesized in-house by reacting methylamine with hydroiodic acid (57%) at a 2.4:1 molar ratio in ambient air. Upon drying at 100 °C, a white powder was formed, which was then redissolved in ethanol and slowly dried to crystallize at 80 °C. This is the "standard" MAI, which was subsequently stored in ambient air. The "dry" MAI underwent an additional vacuum-drying step after this stage—it was heated in a vacuum oven at 50 °C for 24 h and subsequently stored in a nitrogen-filled dry glovebox (H_2O < 0.1 ppm).

The mixed halide perovskite precursor was fabricated by mixing $PbCl_2$ and MAI in a 1:3 molar ratio in DMF to give a 40% solution by weight. This corresponds to 0.88 M $PbCl_2$ and 2.64 M MAI. The dry precursor solution was made up and stored in a nitrogen-filled dry glovebox (H_2O < 0.1 ppm), and the standard solution was stored in ambient air.

Perovskite Film Fabrication. To form perovskite films, initially glass slides were cleaned sequentially with acetone and isopropyl alcohol and then treated with oxygen plasma for 5 min. The perovskite precursors were then spin-coated in the relevant atmosphere (either in a nitrogen-filled glovebox, for the 0% RH samples, or the homemade humidity-controlled chamber in ambient air with humidity regulated by nitrogen flow through a deionized water bubbler) at 2000 rpm for 60 s. The films were then immediately transferred to a hot plate at 90 °C and annealed for 150 min followed by 120 °C for 15 min.

At this point, any post-treatments were carried out: moisture post-treatments were carried out by heating at 90 °C in an atmosphere of 60 ± 5% RH for 30 min or by leaving at room temperature in a 35 ± 5% RH atmosphere for 4 h. Oxygen post-treatment was carried out by heating at 90 °C within a sealed chamber that had been purged with oxygen.

Immediately after treatment, or annealing if untreated, films were spin-coated with PMMA in the relevant humidity atmosphere (nitrogen-filled glovebox for untreated, post-treated, and 0% RH films and humidity-controlled chamber for films annealed in different RH). This forms an effective moisture barrier while measuring—all measurements were carried out in air and then films were stored subsequently in a nitrogen-filled glovebox. We observed little change during repeat measurements over a number of days of measuring and storage, indicating that the PMMA barrier is effective for protection during measuring. PMMA was dissolved in chlorobenzene at 50 mg/mL and spin-coated at 1000 rpm for 45 s.

Photoluminescence Quantum Efficiency. Steady-state photoluminescence quantum efficiency values and steady-state photoluminescence spectra were determined using a 532 nm CW laser excitation source (Suwtech LDC-800) to illuminate a sample in an integrating sphere (Oriel Instruments 70682NS), and the laser scatter and PL were collected using a fiber-coupled detector (Ocean Optics MayaPro). The spectral response of the fiber-coupled detector setup was calibrated using a spectral irradiance standard (Oriel Instruments 63358). PLQE calculations were carried out using established techniques.[43] Unless otherwise stated, the excitation intensity was 180 mW cm^{-2}.

Time-Resolved Photoluminescence. Time-resolved PL measurements were acquired using a time-correlated single-photon counting setup (FluoTime 300, PicoQuant GmbH). Film samples were photoexcited using a 510 nm laser head (LDH-P-C-510, PicoQuant GmbH) pulsed at a repetition rate of 1 MHz, with a pulse duration of 117 ps and fluence of ~3 $\mu J/cm^2$ per pulse. The PL was collected using a high-resolution monochromator and hybrid photomultiplier detector assembly (PMA Hybrid 40, PicoQuant GmbH).

***In Situ* Absorbance.** After spin-coating a perovskite film, the sample was left to dry in an enclosed container for 45 min. During this time, the relative humidity of the glovebox was adjusted by releasing water into the atmosphere. When the correct humidity was reached, the sample was transferred to a hot plate at 90 °C and the absorbance measurement was started immediately. The light source for the absorbance measurement was a halogen light (Philips Brilliantline 14619) incident on the sample at a 60° angle. The light transmitted through the sample is scattered by the white hot plate below the sample. This scattered light is transmitted again through the sample and then collected by a fiber-optic cable, connected to a fiber-optic spectrometer (Avantes Avaspec-2048_14).

Solar Cell Fabrication. For meso-superstructured device fabrication, FTO-coated glass substrates (Pilkington, 7 Ω/□) were first cleaned with detergent and deionized water, then with acetone and isopropyl alcohol, followed by oxygen plasma treatment. The electron-accepting TiO_2 compact layer was spin-coated (2000 rpm for 60 s) from a mildly acidic (after addition of 12 μM HCl) solution of titanium isopropoxide in anhydrous ethanol and sintered at 500 °C. An alumina mesoporous scaffold was then deposited by spin-coating (2500 rpm for 60s) a colloidal dispersion of 20 nm Al_2O_3 nanoparticles in isopropyl alcohol followed by drying at 150 °C. Devices were then transferred into the relevant atmosphere (nitrogen-filled glovebox or humidity-controlled chamber). The perovskite layer was then spin-coated (2000 rpm for 45 s) and annealed at 100 °C

for 120 min. After annealing, any post-treatments were carried out as previously described. Immediately after any treatments, the hole transport layer was deposited by spin-coating in a nitrogen-filled glovebox. For the moisture-blocking SWCNT-HTL, first, the SWNT layer was deposited dynamically by slow drop-by-drop spin-coating (3000 rpm for 90 s) using 200 μL of solution. The SWCNTs were functionalized previously with P3HT as described previously and sonicated and purged with nitrogen before use.[9,35] This layer was followed immediately by the deposition of the PMMA or PC layer (30 mg/mL in chlorobenzene), which had a thickness of ~300 nm. The devices were completed by evaporating silver electrodes with a thickness of 120 nm.

For Spiro-OMeTAD-based devices, instead of the SWCNT and PMMA/PC layers, Spiro-OMeTAD was then deposited *via* spin-coating (at 2000 rpm) a 0.0788 M solution in chlorobenzene with additives of 0.0184 M lithium bis(trifluoromethanesulfonyl)imide (added in 0.61 M acetonitrile solution) and 0.0659 M 4-*tert*-butylpyridine.

For planar devices, the same procedure was carried out, but no mesoporous scaffold was employed and the perovskite layer was annealed as for the films on glass (90 °C for 150 min, then 120 °C for 15 min).

Device Characterization. The current density−voltage ($J-V$) curves were measured (2400 series sourcemeter, Keithley Instruments) under simulated AM1.5 sunlight at 100 mW cm^{-2} irradiance generated by an Abet Class AAB Sun 2000 simulator, with the intensity calibrated with an NREL-calibrated KG5-filtered Si reference cell. The mismatch factor was calculated to be less than 1%. The solar cells were masked with a metal aperture to define the active area of 0.092 cm^{-2} and measured in a light-tight sample holder to minimize any edge effects and to ensure that the reference cell and test cell are located during measurement in the same spot under the solar simulator. For the fast $J-V$ scans, cells were scanned from forward bias to short circuit at a rate of 0.38 V/s after holding under illumination at 1.4 V for 5 s. The maximum power point was determined from these fast $J-V$ scans and current measured holding at this voltage for the stabilized power output measurements.

Film Characterization. A Hitachi S-4300 field emission scanning electron microscope was used to acquire scanning electron microscopy images. A Nikon optical microscope was used to acquire optical micrographs. Sample thicknesses were measured using a Veeco Dektak 150 surface profilometer.

PL Mapping. The photoluminescence maps were recorded using a home-built setup. The modulated pump laser beam (650 nm) was focused onto the sample with submicron resolution using a confocal microscope objective. The transmitted light was recolumnated by a similar objective, collected in an optical fiber, and detected using an InGaAs photodiode. The signal was measured with a lock-in amplifier set to the same frequency and phase as the excitation pump. To collect a map, the sample position was varied with a piezoelectric stage. The excitation intensity was varied from approximately 10^{20} to 2×10^{21} cm^{-2}.

Conflict of Interest: The authors declare no competing financial interest.

Supporting Information Available: The Supporting Information is available free of charge on the ACS Publications website at DOI: 10.1021/acsnano.5b03626.

Device statistics, Spiro-OMeTAD-based devices, PLQE with further annealing, and other supplementary figures and information (PDF)

Acknowledgment. This work was part funded by EPSRC and from the European Union Seventh Framework Programme [FP7/2007-2013] under grant agreement no. 604032 of the MESO project. The work in Eindhoven has received funding from the European Union Seventh Framework Programme [FP7/2007-2013] under grant agreement ERC-2013-ADG no. 339031. G.E. is supported by the EPSRC and Oxford Photovoltaics Ltd. through a Nanotechnology KTN CASE award. R.S. is a Commonwealth Scholar, funded by the UK government. The work of author J.J.F. forms part of the research programme of the Dutch Polymer Institute (DPI), project #734. D.W.D. acknowledges support from a National Science Foundation Graduate Research Fellowship (DGE-1256082). We thank E.J.W. Crossland for useful discussions, and S. Koch for experimental assistance.

REFERENCES AND NOTES

1. Kojima, A.; Teshima, K.; Shirai, Y.; Miyasaka, T. Organometal Halide Perovskites as Visible-Light Sensitizers for Photovoltaic Cells. *J. Am. Chem. Soc.* **2009**, *131*, 6050–6051.
2. Zhou, H.; Chen, Q.; Li, G.; Luo, S.; Song, T. -b.; Duan, H.-S.; Hong, Z.; You, J.; Liu, Y.; Yang, Y. Interface Engineering of Highly Efficient Perovskite Solar Cells. *Science* **2014**, *345*, 542–546.
3. Jeon, N. J.; Noh, J. H.; Yang, W. S.; Kim, Y. C.; Ryu, S.; Seo, J.; Seok, S. Il Compositional Engineering of Perovskite Materials for High-Performance Solar Cells. *Nature* **2015**, *517*, 476–480.
4. You, J.; Yang, Y.; Hong, Z.; Song, T.-B.; Meng, L.; Liu, Y.; Jiang, C.; Zhou, H.; Chang, W.-H.; Li, G.; et al. Moisture Assisted Perovskite Film Growth for High Performance Solar Cells. *Appl. Phys. Lett.* **2014**, *105*, 183902.
5. Pathak, S.; Sepe, A.; Sadhanala, A.; Deschler, F.; Haghighirad, A.; Sakai, N.; Goedel, K. C.; Stranks, S. D.; Noel, N.; Price, M.; et al. Atmospheric Influence upon Crystallization and Electronic Disorder and Its Impact on the Photophysical Properties of Organic−Inorganic Perovskite Solar Cells. *ACS Nano* **2015**, *9*, 2311–2320.
6. Ko, H.-S.; Lee, J.; Park, N. 15.76% Efficiency Perovskite Solar Cells Prepared under High Relative Humidity: Importance of PbI_2 Morphology in Two-Step Deposition of $CH_3NH_3PbI_3$. *J. Mater. Chem. A* **2015**, *3*, 8808–8815.
7. Raga, S. R.; Jung, M.-C.; Lee, M. V.; Leyden, M. R.; Kato, Y.; Qi, Y. Influence of Air Annealing on High Efficiency Planar Structure Perovskite Solar Cells. *Chem. Mater.* **2015**, *27*, 1597–1603.
8. Christians, J. a.; Miranda Herrera, P. A.; Kamat, P. V. Transformation of the Excited State and Photovoltaic Efficiency of $CH_3NH_3PbI_3$ Perovskite upon Controlled Exposure to Humidified Air. *J. Am. Chem. Soc.* **2015**, *137*, 1530–1538.
9. Habisreutinger, S. N.; Leijtens, T.; Eperon, G. E.; Stranks, S. D.; Nicholas, R. J.; Snaith, H. J. Carbon Nanotube/Polymer Composites as a Highly Stable Hole Collection Layer in Perovskite Solar Cells. *Nano Lett.* **2014**, *14*, 5561–5568.
10. Yang, J.; Siempelkamp, B. D.; Liu, D.; Kelly, T. L. Investigation of $CH_3NH_3PbI_3$ Degradation Rates and Mechanisms in Controlled Humidity Environments Using in Situ Techniques. *ACS Nano* **2015**, *9*, 1955–1963.
11. Leguy, A.; Hu, Y.; Campoy-Quiles, M.; Alonso, M. I.; Weber, O. J.; Azarhoosh, P.; van Schilfgaarde, M.; Weller, M. T.; Bein, T.; Nelson, J.; et al. Reversible Hydration of $CH_3NH_3PbI_3$ in Films, Single Crystals and Solar Cells. *Chem. Mater.* **2015**, *27*, 3397–3407.
12. Bass, K. K.; McAnally, R. E.; Zhou, S.; Djurovich, P. I.; Thompson, M.; Melot, B. Influence of Moisture on the Preparation, Crystal Structure, and Photophysical Properties of Organohalide Perovskites. *Chem. Commun.* **2014**, *50*, 15819–15822.
13. Suarez, B.; Gonzalez-Pedro, V.; Ripolles, T. S.; Sánchez, R. S.; Otero, L. A.; Mora-Sero, I. Recombination Study of Combined Halides (Cl, Br, I) Perovskite Solar Cells. *J. Phys. Chem. Lett.* **2014**, *5*, 1628–1635.
14. Zhang, W.; Saliba, M.; Moore, D. T.; Pathak, S. K.; Hörantner, M. T.; Stergiopoulos, T.; Stranks, S. D.; Eperon, G. E.; Alexander-Webber, J. A.; Abate, A.; et al. Ultrasmooth Organic−inorganic Perovskite Thin-Film Formation and Crystallization for Efficient Planar Heterojunction Solar Cells. *Nat. Commun.* **2015**, *6*, 6142.
15. Williams, S. T.; Zuo, F.; Chueh, C.-C.; Liao, C.-Y.; Liang, P.-W.; Jen, A. K.-Y. Role of Chloride in the Morphological Evolution of Organo-Lead Halide Perovskite Thin Films. *ACS Nano* **2014**, *8*, 10640–10654.
16. Grancini, G.; Marras, S.; Prato, M.; Giannini, C.; Quarti, C.; De Angelis, F.; De Bastiani, M.; Eperon, G. E.; Snaith, H. J.; Manna, L.; et al. The Impact of the Crystallization Processes on the Structural and Optical Properties of

Hybrid Perovskite Films for Photovoltaics. *J. Phys. Chem. Lett.* **2014**, *5*, 3836–3842.
17. Dar, M. I.; Arora, N.; Gao, P.; Ahmad, S.; Grätzel, M.; Nazeeruddin, M. K. Investigation Regarding the Role of Chloride in Organic–Inorganic Halide Perovskites Obtained from Chloride Containing Precursors. *Nano Lett.* **2014**, *14*, 6991–6996.
18. Zheng, L.; Zhang, D.; Ma, Y.; Lu, Z.; Chen, Z.; Wang, S.; Xiao, L.; Gong, Q. Morphology Control of the Perovskite Films for Efficient Solar Cells. *Dalt. Trans.* **2015**, *44*, 10582–10593.
19. Eperon, G. E.; Burlakov, V. M.; Docampo, P.; Goriely, A.; Snaith, H. J. Morphological Control for High Performance, Solution-Processed Planar Heterojunction Perovskite Solar Cells. *Adv. Funct. Mater.* **2014**, *24*, 151–157.
20. Liang, P.-W.; Liao, C.-Y.; Chueh, C.-C.; Zuo, F.; Williams, S. T.; Xin, X.-K.; Lin, J.; Jen, A. K.-Y. Additive Enhanced Crystallization of Solution-Processed Perovskite for Highly Efficient Planar-Heterojunction Solar Cells. *Adv. Mater.* **2014**, *26*, 3748–3754.
21. Tan, K. W.; Moore, D. T.; Saliba, M.; Sai, H.; Estroff, L. a.; Hanrath, T.; Snaith, H. J.; Wiesner, U. Thermally Induced Structural Evolution and Performance of Mesoporous Block Copolymer-Directed Alumina Perovskite Solar Cells. *ACS Nano* **2014**, *8*, 4730–4739.
22. Saliba, M.; Tan, K. W.; Sai, H.; Moore, D. T.; Scott, T.; Zhang, W.; Estroff, L. a.; Wiesner, U.; Snaith, H. J. The Influence of Thermal Processing Protocol upon the Crystallization and Photovoltaic Performance of Organic-Inorganic Lead Trihalide Perovskites. *J. Phys. Chem. C* **2014**, *118*, 17171–17177.
23. Moore, D. T.; Sai, H.; Tan, K. W.; Estroff, L. a.; Wiesner, U. Impact of the Organic Halide Salt on Final Perovskite Composition for Photovoltaic Applications. *APL Mater.* **2014**, *2*, 81802.
24. Yang, W. S.; Noh, J. H.; Jeon, N. J.; Kim, Y. C.; Ryu, S.; Seo, J.; Seok, S. I. High-Performance Photovoltaic Perovskite Layers Fabricated through Intramolecular Exchange. *Science* **2015**, *348*, 1234–1237.
25. Wu, Y.; Islam, A.; Yang, X.; Qin, C.; Liu, J.; Zhang, K.; Peng, W.; Han, L. Retarding the Crystallization of PbI_2 for Highly Reproducible Planar-Structured Perovskite Solar Cells *via* Sequential Deposition. *Energy Environ. Sci.* **2014**, *7*, 2934.
26. Dualeh, A.; Tétreault, N.; Moehl, T.; Gao, P.; Nazeeruddin, M. K.; Grätzel, M. Effect of Annealing Temperature on Film Morphology of Organic-Inorganic Hybrid Pervoskite Solid-State Solar Cells. *Adv. Funct. Mater.* **2014**, *24*, 3250–3258.
27. Unger, E. L.; Bowring, A. R.; Tassone, C. J.; Pool, V.; Gold-Parker, A.; Cheacharoen, R.; Stone, K. H.; Hoke, E. T.; Toney, M. F.; McGehee, M. D. Chloride in Lead-Chloride Derived Organo-Metal Halides for Perovskite-Absorber Solar Cells. *Chem. Mater.* **2014**, *26*, 7158–7165.
28. Eperon, G. E.; Burlakov, V. M.; Goriely, A.; Snaith, H. J. Neutral Color Semitransparent Microstructured Perovskite Solar Cells. *ACS Nano* **2014**, *8*, 591–598.
29. Burlakov, V. M.; Eperon, G. E.; Snaith, H. J.; Chapman, S. J.; Goriely, A. Controlling Coverage of Solution Cast Materials with Unfavourable Surface Interactions. *Appl. Phys. Lett.* **2014**, *104*, 091602.
30. Stranks, S. D.; Burlakov, V. M.; Leijtens, T.; Ball, J. M.; Goriely, A.; Snaith, H. J. Recombination Kinetics in Organic-Inorganic Perovskites: Excitons, Free Charge, and Subgap States. *Phys. Rev. Appl.* **2014**, *2*, 34007.
31. de Quilettes, D. W.; Vorpahl, S. M.; Stranks, S. D.; Nagaoka, H.; Eperon, G. E.; Ziffer, M. E.; Snaith, H. J.; Ginger, D. S. Impact of Microstructure on Local Carrier Lifetime in Perovskite Solar Cells. *Science* **2015**, *348*, 683–686.
32. D'Innocenzo, V.; Srimath Kandada, A. R.; De Bastiani, M.; Gandini, M.; Petrozza, A. Tuning the Light Emission Properties by Band Gap Engineering in Hybrid Lead-Halide Perovskite. *J. Am. Chem. Soc.* **2014**, *136*, 17730–17733.
33. Chen, Q.; Zhou, H.; Song, T.-B.; Luo, S.; Hong, Z.; Duan, H.-S. S.; Dou, L.; Liu, Y.; Yang, Y. Controllable Self-Induced Passivation of Hybrid Lead Iodide Perovskites toward High Performance Solar Cells. *Nano Lett.* **2014**, *14*, 4158–4163.
34. Abate, A.; Leijtens, T.; Pathak, S.; Teuscher, J.; Avolio, R.; Errico, M. E.; Kirkpatrik, J.; Ball, J. M.; Docampo, P.; McPherson, I.; et al. Lithium Salts as "Redox Active" P-Type Dopants for Organic Semiconductors and Their Impact in Solid-State Dye-Sensitized Solar Cells. *Phys. Chem. Chem. Phys.* **2013**, *15*, 2572–9.
35. Habisreutinger, S. N.; Leijtens, T.; Eperon, G. E.; Stranks, S. D.; Nicholas, R. J.; Snaith, H. J. Enhanced Hole Extraction in Perovskite Solar Cells Through Carbon Nanotubes. *J. Phys. Chem. Lett.* **2014**, *5*, 4207–4212.
36. Rau, U. Reciprocity Relation between Photovoltaic Quantum Efficiency and Electroluminescent Emission of Solar Cells. *Phys. Rev. B: Condens. Matter Mater. Phys.* **2007**, *76*, 1–8.
37. Tvingstedt, K.; Malinkiewicz, O.; Baumann, A.; Deibel, C.; Snaith, H. J.; Dyakonov, V.; Bolink, H. J. Radiative Efficiency of Lead Iodide Based Perovskite Solar Cells. *Sci. Rep.* **2014**, *4*, 1–7.
38. Nguyen, W. H.; Bailie, C. D.; Unger, E. L.; McGehee, M. D. Enhancing the Hole-Conductivity of Spiro-OMeTAD without Oxygen or Lithium Salts by Using spiro(TFSI)2 in Perovskite and Dye-Sensitized Solar Cells. *J. Am. Chem. Soc.* **2014**, *136*, 10996–11001.
39. Deschler, F.; Price, M.; Pathak, S.; Klintberg, L.; Jarausch, D. D.; Higler, R.; Huettner, S.; Leijtens, T.; Stranks, S. D.; Snaith, H. J.; et al. High Photoluminescence Efficiency and Optically-Pumped Lasing in Solution-Processed Mixed Halide Perovskite Semiconductors. *J. Phys. Chem. Lett.* **2014**, *5*, 1421–1426.
40. Xiao, Z.; Dong, Q.; Bi, C.; Shao, Y.; Yuan, Y.; Huang, J. Solvent Annealing of Perovskite-Induced Crystal Growth for Photovoltaic-Device Efficiency Enhancement. *Adv. Mater.* **2014**, *26*, 6503–6509.
41. Noel, N. K.; Abate, A.; Stranks, S. D.; Parrott, E. S.; Burlakov, V. M.; Goriely, A.; Snaith, H. J. Enhanced Photoluminescence and Solar Cell Performance *via* Lewis Base Passivation of Organic–Inorganic Lead Halide Perovskites. *ACS Nano* **2014**, *8*, 9815–9821.
42. Abate, A.; Saliba, M.; Hollman, D. J.; Stranks, S. D.; Wojciechowski, K.; Avolio, R.; Grancini, G.; Petrozza, A.; Snaith, H. J. Supramolecular Halogen Bond Passivation of Organic–Inorganic Halide Perovskite Solar Cells. *Nano Lett.* **2014**, *14*, 3247–3254.
43. de Mello, J. C.; Wittmann, H. F.; Friend, R. H. An Improved Experimental Determination of External Photoluminescence Quantum Efficiency. *Adv. Mater.* **1997**, *9*, 230.